INTERNATIONAL JOURNAL OF ENGINEERING
AND APPLIED SCIENCE
ISSN 2709-8117
JUN. 2021 VOL. 2, NO. 2

Studies on the Electronic and Optical Properties of WSXSe2−x (0≤x≤2) in Bulk and Monolayer Configurations

Iftikhar Almanna Lubis
Department of Physics, Razi University, Kermanshah, Iran

ABSTRACT

The purpose of this study was to explore the effects of enzymes, probiotics and their combinations on intestinal histopathological indexes of broilers. One hundred and fifty broilers were randomly assigned to five diet groups for 42 days. We measured the performance indicators of five treatment groups. On the 42nd day, 2 chickens per replicate were collected for microbe count, and about 5cm of the distal ileum was resected for histopathological examination. The results showed that the total heterotrophic count of the basal diet and the probiotics diet was similar to that of the other diets, but significantly (P <0.05) higher than that of the other diets. The lactic acid bacteria count was the highest in the probiotics + enzyme feed, and the lowest in the probiotics (2.58×105 CFU/mL) and enzyme supplemented feed (1.45×105 CFU/mL). The total coliform number of antibiotic diet (14.12×105 CFU/mL) was significantly lower than that of other diets (P <0.05). The total number of Escherichia coli was the highest in the antibiotic diet and the lowest in the probiotics + enzyme mixture diet. Micrograph of ileum under basal diet showed mucosal shedding and villi degeneration. In this experiment, the supplementation of probiotics, enzymes or their combinations had no significant effects on the growth response of broilers. However, the birds' gut integrity was improved. In poultry nutrition, a mixture of 0.4% probiotics plus 0.1% enzymes is recommended as an alternative to antibiotic growth promoters.

KEYWORDS

Tungsten sulphoselenide; Optical properties; Electronic properties; Density functional theory; Band gap.

1. Introduction

Recently, two-dimensional transition metal dichalcogenides (TMDCs) such as MoS2, MoSe2, WS2 and WSe2 have attracted researchers attention due to their layered structure, unique electronic and optical properties, and their potential applications in nanosystems[1-6]. Unlike the semi-metal graphene with zero band gap,

these materials have direct band gap in mono-layer case, in which the valence band maximum (VBM) and the conduction band minimum (CBM) are placed at the K (K ′) point of the hexagonal Brilouin zone[7-12]. Bulk 2H–MoS2 is, in general, a p-type semiconductor and is resistant to oxidation. It is used as a solid lubricant or a catalyst in industry[13]. Similar to graphene and H-BN, 2D-TMDCs are made not only by mechanical and chemical laminating of layered bulk counterparts but also directly by the chemical vapor deposition (CVD) or two-step thermolysis[14-20]. Just like their bulk counterparts, these 2D materials have different electronic properties covering superconductors[21-22], metals[23], insulators[24], and wide band gap semiconductors[25-26]. In these structures, due to the layered structure and the existence of a wide band gap, it is possible to form layered compounds with different atoms and molecules between the layers of transition metal dichalcogenides[27]. Moreover, various nano-electronic and photonics applications have been proposed for these 2D materials[28-30]. In order to control the band gap of these materials for the construction of optoelectronic devices, researchers have mixed semiconductors with different band gaps and similar atomic structures and thus, they achieved mixed alloy systems with tunable band gap. The acquisition of semiconductor nanostructures with adjustable band gap for applications in nano-electronics and nano-photonics is very important. Recent developments in 0D, 1D semiconductor structures have shown that their band gap and light emission can be slowly adjusted by changing their constituent stoichiometries[31]. However, such studies have been less done on thin 2D systems. Theoretical calculations have shown that 2D alloys, such as mixed ternary compounds of MoS2, MoSe2, and MoTe2 are thermodynamically stable at room temperature and the properties of their compositions can be regulated steadily between their component parts[32]. In this study, a systematic approach is considered to gain insight into the electronic and optical properties of layered Tungsten sulphoselenide WSxSe2−x ($0 \leqslant x \leqslant 2$).

2. Computational Method

All calculations presented in this study were performed using the fullpotentialaugmentedplane-wavepluslocalorbital(FPLAPW+lo) method in the frame work of the density functional theory (DFT)[33] as implemented in WIEN2k code[34]. Investigations of electronic and optical properties are relatively performed. Two types of exchangecorrelation (XC) potentials, the Perdew-Burke-Ernzerhof (PBE)[35] functional form of the generalized gradient approximation(GGA) and the Engel–Vosko scheme of the generalized gradient approximation (GGA) were applied in the calculations. The supercells were used to simulate isolated sheets and in order to avoid interlayer interactions, the distance between sheets was considered to be larger than 15Å. The structuresarefullyrelaxeduntilallforcesarelessthan0.003eV/A.The convergence parameter RminMT Kmax (i.e. the product of the smallest of atomic sphere radii RMT and the plane-wave cut off parameter Kmax, which controls the size of the basis set in these calculations) was set to 8. The maximum l quantum number for the wave-function expansion inside the atomic sphere was confined to lmax = 10. The Gmax parameter was considered to be 14 Ry. Brillouin zone k-point integrations were performed using the tetrahedron method [36] on a grid of 208 k-points in the irreducible part of the hexagonal

Brillouin zone, which corresponds to 1000 k-points throughout the Brillouin zone. However, for the determination of optical properties, a denser sampling of the Brillouin zone was needed where we used 8000 k-points throughout the Brillouin zone(33×33×7). The energy convergence of 10−4 Ry and charge convergence of 10−3 e were selected. All these values were selected in such a way to ensure the convergence of the results.

Transition metals dichalcogenide (TMDC) are layered compounds in which X-M-X atoms are attached together in each layer with strong covalent bonds, and each layer with its adjacent layer has a weak Vander Waals bond. In mono-layer case, the transition metal dichalcogenide (TMDC) consists of a hexagonal arrangement of transition metals (M = Ti, Nb, Ta, Mo, W) which is sandwiched between two layers of chalcogen atoms (X = S, Se, Te) [27].

3. Electronic Properties

Here, in order to study the electronic properties of WSxSe2−x (0⩽x⩽2), we investigate the total density of states and the effective orbitals using two functionals of GGA and GGA-EV in the bulk and mono-layer cases. Fig.1 shows the total electronic density of states for these compounds in the two cases of bulk and mono-layer using the GGA exchange correlation potential. Because of the last orbital of Se atom is 4p4 and the last orbital of S atom is 3p4 and since the energy of 4p4 is greater than 3p4, we expect that band gap of WSe2 is smaller than two other compounds which is in agreement with our results. As can be seen in the density of states (DOS) with increasing the density of Se atoms (in the both bulk and mono-layer cases), the energy gap decreases which this decrement is more significant in the mono-layer case. Also, the energy gap increases by converting the material from bulk to mono-layer. A remarkable point among all these semiconductor compounds is that all of them are p-type semiconductors promising to use these materials in spintronics and thermoelectrics. In Fig.2 and Fig.3, respectively, we can find the d orbital of W atom and the p orbitals of chalcogen atoms (S, Se) in both bulk and mono-layer cases. W atom has an electronic configuration (74W: [54Xe] 6s2,5d4) and its valence band ends in the d orbital and chalcogen atoms (S, Se) with the electronic configuration 16S: [10Ne] 3s2, 3p4 and 34Se: [18Ar] 4s2, 3d10, 4p4, respectively, hence, their valence band end with the p orbitals; this is the reason for the formation of strong covalent bonds between them. Investigating the partial density of states (PDOS) show that the W-5d and S-3p atomic orbitals will play a decisive role in the properties of WS2. Our PDOS (Fig.2 and Fig.3) shows that the major contribution in the valence (and conduction) band in bulk and mono-layer WS2 comes from chalcogen atoms (S, Se) p orbitals and Tungsten d orbitals. Around the Fermi level in the valence region, the portion of p and d orbitals are approximately equal in the both bulk and mono-layer cases. The most difference in the electronic density of states is observed in the conduction region. In this region, the portion of d orbital is extremely more than the portion of p orbitals of the chalcogen atoms (S, Se) in both bulk and mono-layer cases.

In both bulk and mono-layer cases, by increasing the density of the Se atom, the variation in the density of states is approximately the same in both valence and conduction regions for these compounds. For example, in the conduction region of WSSe compound, the intensity of the density of states and also its width decrease, while in the conduction region of WSe2, two sharp peaks are created (the peaks become more localized).
In Fig.4, the total band structure of WS2 in bulk and monolayer cases are presented. As can be seen in both cases, the systems shows a semiconducting properties. Another interesting point in these band structures is that the population of bands in monolayer case decreases in comparison with bulk case which indicates decreasing conducting property in this case and increasing the band-gap.

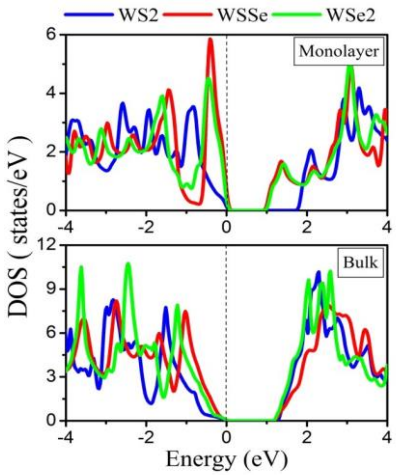

Figure1. Total density of states for the monolayer (upper panel) and bulk (lower panel) Tungsten sulphoselenide WSxSe2−x (0⩽x⩽2)

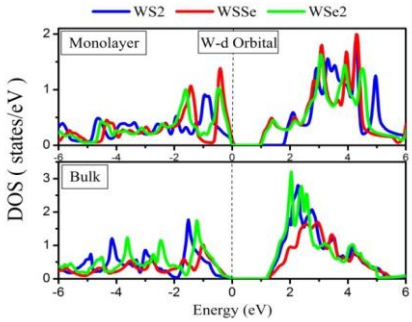

Figure 2. Atomic projected density of states of Tungsten d orbitals for the monolayer (upper panel) and bulk (lower panel) Tungsten sulphoselenide WSxSe2−x (0⩽x⩽2)

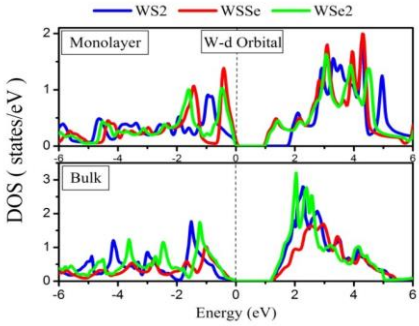

Figure 3. Atomic projected density of states of Chalcogen atoms (S, Se) p orbitals for monolayer (upper panel) and bulk (lower panel) Tungsten sulphoselenide WSxSe2−x (0⩽x⩽2)

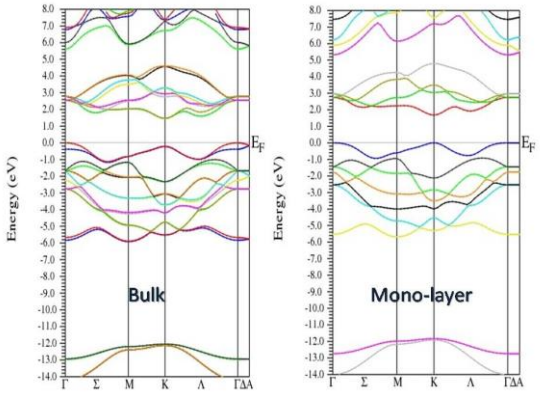

Figure 4. Total band structure of Bulk and Mono-layer of WS2

In most of the semiconductors, the theoretical (GGA) energy band gaps are underestimated as compared to the experimental results. The Engel–Vosko gives improved band gap as compare to GGA and in close agreement with the experimental results. As shown in Table 1, the variation of the exchange-correlation potential has the maximum and minimum effects on the bulk WS2 and the mono-layer WSe2 respectively.

4. Optical Properties

Having the real and imaginary parts of the dielectric function and based on the Kramers-Kronig relations, $\varepsilon(\omega) = \varepsilon 1(\omega) + \varepsilon 1(\omega)$, one can obtain optical constants such as reflection and the spectrum of loss function. The real part of dielectric function, $\varepsilon 1(\omega)$, represents the response of the material to the incident photon, which, in our structures, due to the geometric symmetry in the two directions of x and y, we study the optical properties

along the x direction (on plane) and the z direction (perpendicular to plane). Fig.5 shows the real part of dielectric function, ε1(ω), for the both bulk and mono-layer WSxSe2−x (0⩽x⩽2) compounds in two x and z directions. The static values of the real part of the dielectric function and its roots in both bulk and mono-layer cases for x and z directions are listed in table 2. As can be seen, the static value for the WS2 compound is smaller than the other two compounds, which means that the conductivity and the band gap of this compound is less and wider than the other two compounds respectively.

In the bulk case, and for both directions, the static value for WSSe, WSe2 is approximately equal, while for the mono-layer, static value for WSSe and WS2 are more closer. According to Table 2, the most conductivity property is associated with the x direction in the bulk case of these compounds and the least conductivity property is related to their z direction in mono-layer case. For all three compounds, by increasing the energy of the incident photon, we see a sharp Dirac peak around the edge of the visible area in bulk case along x direction, and then a sudden drop happens, indicating that the response is not stable at the edge of the visible area. In the next step, with increasing the intensity of the incident photon, from the edge of the ultraviolet region until about 8eV the real part of the dielectric function, ε1(ω), becomes negative, so in this region there is basically no response to the incident photon and the material exhibits a strong reflectivity. Also, energy loss is observed only in this area. From 8eV to 11.5eV, there is a small peak indicating a small response, and then, again, there are no responses. However, in z direction for the bulk case, the response is less intense and more wider than along the x direction in the visible area. In this latter case, we also observe a blue shift. In the case of mono-layer, the intensity of response to the incident photon in both directions is less than the corresponding one in the bulk case. Along x direction in the infrared region, the first response to the incident photon is connected to WSe2, but the other two compounds respond to the incident photon at the edge of the visible area, where, the response rate of WSSe, unlike its bulk case, is less than the other two compounds. In z direction, the first responses of all three structures occur in the visible area, which may be very useful for the solar cell industry.

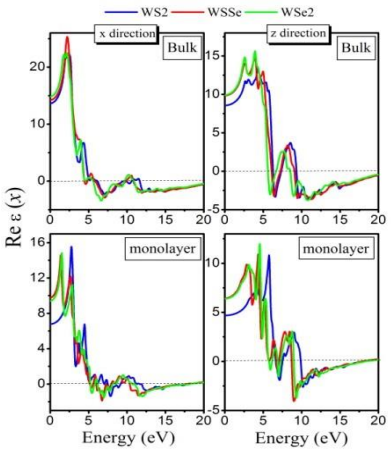

Figure 5. The real part of dielectric function for bulk (upper panel) and monolayer (lower panel) Tungsten sulphoselenide WSxSe2−x (0⩽x⩽2) in x and z directions

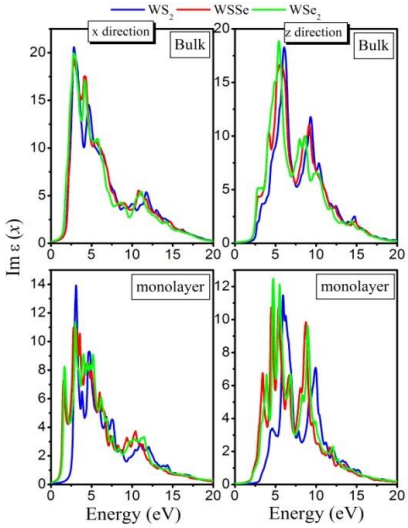

Figure 6. The imaginary part of dielectric function for bulk (upper panel) and monolayer (lower panel) Tungsten sulphoselenide WSxSe2−x (0⩽x⩽2) in x and z directions

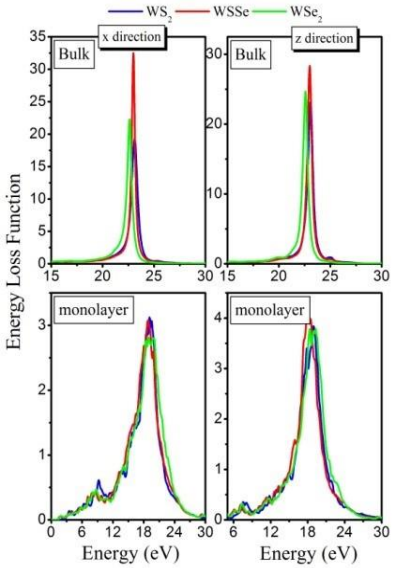

Figure 7. The calculated energy loss function, L(ω), for the bulk (upper panel) and monolayer (lower panel) Tungsten sulphoselenide WSxSe2−x (0⩽x⩽2) in x and z directions

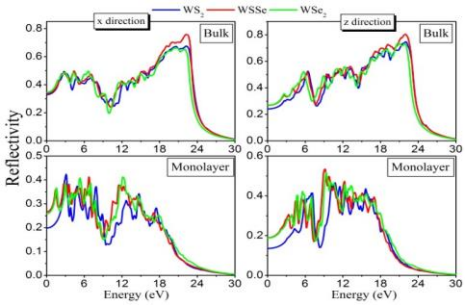

Figure 8. The calculated frequency-dependent reflectivity, for bulk (upper panel) and monolayer (lower panel) Tungsten sulphoselenide WSxSe2−x (0⩽x⩽2) in both x and z directions

The imaginary part of the dielectric function represents the electron transition from the valence band to the conduction band, which determines whether it is conductor or semiconducting. Fig.6 shows the imaginary

part of the dielectric function in two x and z directions for the above-mentioned compounds. For all of these structures, and in the infrared region until the edge of visible area, we almost see optical gaps corresponding to the electronic band gaps (Table 1), which this correspondence is more observed along x direction. By increasing the energy of incident photon in the bulk case and along the x direction, we see a sharp Dirac peak in the edge of the visible area, which is more intense for WS2 than the other two compounds. However, along z direction and in the ultraviolet region, after a few relatively weak transitions in the visible area, the main transition occurs near the edge of the ultraviolet region. Some transitions are observed at higher energies as well, which along x and z directions, these peaks correspond to the transitions from the p orbital of the chalcogen atoms to the d orbital of the transition metal atoms. But in the case of the mono-layer and along x direction, the first main transition is related to WSe2 placed in the infrared region, and the main transitions of the two other compounds occur in the visible area. In the energies of 4eV and 10eV, we see other transitions in this direction. In the z direction, the first major transition occurs in WSSe at the edge of the ultraviolet region, and for the two other compounds, these transitions occurs in the ultraviolet region; also by increasing the energy of the incident photon, some peaks are observed in the range of 8-10eV. The interesting point about these structures is that the diagrams show a blue shift in the z direction relative to x direction. z directions. The main energy dissipation in the matter is due to the oscillations of plasmons forming standing waves, and therefore the incident photon do not recieve a response from the environment. In the bulk case along x direction, as an example, we see a sharp peak in the energy range between 5-8 eV, which is precisely the same as the forbidden region (the range of energies corresponding to the negative values of $\varepsilon 1(\omega)$), which is evident in other graphs as well. In confirmation of the previous argument, it is seen that the reflection coefficient in Fig.8 shows a semi-conducting behavior, so that in the static state, the maximum reflection coefficient is related to the x direction in the bulk case with an approximate value of 35%, and the lowest reflection coefficient is related to z direction in the mono-layer case with approximately 15% to 20%. In all of these compounds, in the bulk and mono-layer cases, and in both x and z directions, WSe2 and WS2 have the highest and the lowest reflection coefficient. In the range of higher energies, for both directions, the reflection coefficient in the bulk case is bigger than the mono-layer one, which means that in the bulk case, the metallic behavior in the high energy range is more than the mono-layer one.

5. Conclusions

In summary, we investigated the electronic and optical properties of Tungsten sulphoselenide WSxSe2−x ($0 \leqslant x \leqslant 2$) in both bulk and monolayer forms by utilizing ab initio calculations. In terms of electronic properties, with increasing the density of Se atom, the energy gap decreases, so that the reduction of the band gap in the mono-layer is more observable than the bulk case. The major effect on the variation in electronic states is connected to the transitions from d orbital of W atom to p orbitals of chalcogen atoms (S, Se). Changing the exchange-correlation potential has the maximum and

References

U. Halim, C.R. Zheng, Y. Chen, Z. Lin, S. Jiang, R. Cheng, Y. Huang, X. Duan: "A rational design of cosolvent exfoliation of layered materials by directly probing liquid-solid interaction", Nat. Comm, 2013, 4, pp. 2213.

W. J. Yu, Y. Liu, H. Zhou, A. Yin, Z. Li, Y. Huang, X. Duan: "Highly efficient gatetunable photocurrent generation in vertical heterostructures of layered materials", Nat. Nanotechnol, 2013, 8, pp. 952-958.

W. J. Yu, Z. Li, H. Zhou, Y. Chen, Y. Wang, Y. Huang, X. Duan: "Vertically stacked multi-heterostructures of layered materials for logic transistors and complementary inverters", Nat. Mater, 2013, 12, pp. 246-252.

H. Qiu, T. Xu, Z. Wang, W. Ren, H. Nan, Z. Ni, Q. Chen, S. Yuan, F. Miao, F. Song, G. Long, Y. Shi, L. Sun, J. Wang, X. Wang: "Hopping transport through defect-induced localized states in molybdenum disulphide", Nat. Comm, 2013, 4, pp. 2642.

X. Luo, Y. Zhao, J. Zhang, M. Toh, C. Kloc, Q. Xiong, S. Y. Quek: "Effects of lower symmetry and dimensionality on Raman spectra in two-dimensional WSe2", Phys. Rev, 2013, 88, pp. 195313.

A. Jones, H. Yu, N. Ghimire, S. Wu, G. Aivazian, J. Ross, B. Zhao, J. Yan, D. Mandrus, D. Xiao, W. Yao, X. Xu: "Optical generation of excitonic valley coherence in monolayer WSe2", Nat. Nanotechnol, 2013, 8, pp. 634-638.

S. Tongay, J. Zhou, C. Ataca, K. Lo, T. S. Matthews, J. Li, J. C. Grossman, J. Wu: "Thermally Driven Crossover from Indirect toward Direct Bandgap in 2D Semiconductors: MoSe2 versus MoS2", Nano Lett, 2012, 12, pp. 5576-5580.

C. Ataca, H. Sahin, S. Ciraci: "Stable, Single-Layer MX2 Transition-Metal Oxides and Dichalcogenides in a Honeycomb-Like Structure", J. Phys. Chem, 2012, 116, pp. 8983-8999.

K. S. Novoselov, A. K. Geim, S. V. Morozov, D. Jiang, Y. Zhang, S. V. Dubonos, I. V. Grigorieva, A. A. Firsov: 'Electric Field Effect in Atomically Thin Carbon Films', Science, 2004, 306, pp. 666-669.

Y. Ding, Y. Wang, J. Ni, L. Shi, S. Shi, W. Tang: "First principles study of structural, vibrational and electronic properties of graphene-like MX2 (M=Mo, Nb, W, Ta; X=S, Se, Te) monolayers", Physica B, 2011, 406, pp. 2254-2260.

K. F. Mak, C. Lee, J. Hone, J. Shan, T. F. Heinz: "Atomically Thin MoS2: A New Direct-Gap Semiconductor", Phys. Rev. Lett, 2010, 105, pp. 136805.

J. Kang, S. Tongay, J. Li, J. Wu: "Monolayer semiconducting transition metal dichalcogenide alloys: Stability and band bowing", Journal of Applied Physics, 2013, 113, pp. 143703.

A. Ayari, E. Cobas, O. Ogundadegbe, M. S. Fuhrer: "Realization and electrical characterization of ultrathin crystals of layered transition-metal dichalcogenides", J. Appl. Phys, 2007, 101, pp. 014507.

K. S. Novoselov, D. Jiang, F. Schedin, T. J. Booth, V. V. Khotkevich, S. V. Morozov, A. K. Geim: "Two-dimensional atomic crystals", PNAS, 2005, 102, pp. 10451-10453.

B. Radisavljevic, A. Radenovic, J. Brivio, V. Giacometti, A. Kis: "Single-layer MoS2 transistors", Nature Nanotech, 2011, 6, pp. 147-150.

G.Eda, H. Yamaguchi, D. Voiry, T. Fujita, M. Chen, M.Chhowalla: "Photoluminescence from Chemically Exfoliated MoS2", Nano Lett, 2011, 11, pp. 5111-5116.

J. N. Coleman, M. Lotya, A. O'Neill, S.D. Bergin, P.J. King, U. Khan, K. Young, A. Gaucher,S.De,R.J.Smith,I.V.Shvets,S.K.Arora,G.Stanton,H.Y.Kim,K.Lee,G.T. Kim,G.S. Duesberg,T. Hallam,J.J. Boland,J.J. Wang,J.F. Donegan,J.C.Grunlan, G. Moriarty,A. Shmeliov,R.J. Nicholls,J.M. Perkins,E.M. Grieveson,K. Theuwissen,D.W. McComb, P.D. Nellist, V. Nicolosi: 'Two-Dimensional Nanosheets Produced by Liquid Exfoliation of Layered Materials', Science, 2011, 331, pp. 568571.

D. Kim, D. Sun, W. Lu, Z. Cheng, Y.Zhu, D. Le,T. S. Rahman, L.Bartels: "Toward the Growth of an Aligned Single-Layer MoS2 Film", Langmuir, 2011, 27, pp. 1165011653.

Y. Zhan, Z. Liu, S. Najmaei, P.M. Ajayan,J. Lou: "Large-Area Vapor-Phase Growth and Characterization of MoS2 Atomic Layers on a SiO2 Substrate", Small, 2012, 8, pp. 966-971.

Y. H.Lee, X.Q.Zhang, W. Zhang, M. T. Chang, C. T. Lin, K. D. Chang, Y. C. Yu, J. T. W. Wang, C. S. Chang, L. J. Li, T.W.Lin: "Synthesis of Large-Area MoS2 Atomic Layers with Chemical Vapor Deposition", Adv. Mat, 2012, 24, pp. 2320-2325.

A. M. Gabovich, A. I. Voitenko, J. F. Annett, M. Ausloos: "Charge—and spindensity-wave superconductors", Supercond. Sci. Tech, 2001:14.

Y. H.Lee, X.Q.Zhang, W. Zhang, M. T. Chang, C. T. Lin, K. D. Chang, Y. C. Yu, J. T. W. Wang, C. S. Chang, L. J. Li, T.W.Lin: "Synthesis of Large-Area MoS2 Atomic Layers with Chemical Vapor Deposition", Adv. Mat, 2012, 24, pp. 2320-2325.

Copyrights